ELSEVIER

Biochimica et Biophysica Acta 1464 (2000) 113–126

BIOCHIMICA ET BIOPHYSICA ACTA
BBA

www.elsevier.com/locate/bba

Submolecular organization of DMPA in surface monolayers: beyond the two-layer model

Manfred Schalke, Peter Krüger, Markus Weygand, Mathias Lösche *

Institute of Experimental Physics I, Leipzig University, Linnéstr. 5, D-04103 Leipzig, Germany

Received 9 September 1999; received in revised form 15 November 1999; accepted 13 December 1999

Abstract

A new approach to the data refinement of X-ray reflection measurements from lipid surface monolayers, applied to DMPA on pure water, reveals the structural organization of the lipid in unprecedented detail and provides new insights into headgroup conformation and hydration as a function of lateral pressure. While conventional box models are incapable of modeling the experimental data at high momentum transfer satisfactorily, a quasimolecular composition–space refinement approach using distribution functions to map the spatial organization of submolecular headgroup fragments yields a much better description and overcomes inherent difficulties of box models. Upon going from the fluid liquid-expanded (LE) phase to the hexatic liquid-condensed (LC) phase, the orientation of the headgroup is tightly coupled to the ordering of the acyl chains. Headgroups tilt toward the surface normal to accommodate for the large reduction in available area per lipid molecule. The spread of the headgroup fragment distribution is considerably larger than the global interface roughness and increases slightly with compression. In distinction to earlier work on DMPE using the two-box approach, we find that the phosphate hydration stays essentially constant across the whole isotherm. The discrepancy between the results observed with the different models is attributed to intrinsic deficiencies of the box model.

Keywords: Langmuir monolayer; Dimyristoylphosphatidic acid; X-ray reflectivity; Headgroup conformation; Headgroup hydration

1. Introduction

Lipid monolayers on aqueous subphases have been intensively studied in recent years with both technological and biomimetic aims in mind [1–3]. Such systems show interesting ordering phenomena on the mesoscopic scale [4,5], and their submolecular organization has been studied with scattering [6,7] and spectroscopic [8] methods. Particularly well understood is the structure formation with respect to the aliphatic chains [9], for which a wealth of information has been obtained using grazing incidence X-ray diffraction (GIXD) [10]. Less well-characterized is the role and the behavior of the hydrophilic lipid headgroups because they do not participate in the hexatic or crystalline ordering which the chains adopt at high two-dimensional molecular density and are thus not amenable to characterization by diffraction methods. They may, however, be characterized in reflectivity measurements using X-rays or neutrons [10–13]. Much more is known on the con-

* Corresponding author. Fax: +49 (341) 97-32-479; E-mail: loesche@physik.uni-leipzig.de

0005-2736/00/$ – see front matter
PII: S0005-2736(99)00249-7

formations of phospholipid headgroups in bilayer systems [14,15]. Moreover, substantial progress has recently been made in the characterization of lipid headgroups in bilayer systems in both Monte-Carlo [16,17] and molecular dynamics [18,19] simulation work. Most recently, modern solid state NMR methods have provided new insights into phospholipid membrane structure from the mapping of the dynamics of atomic contacts [20].

If monolayers are regarded as model systems for biomembranes in biophysical studies, the lipid headgroups are of particular interest, since they constitute the interaction sites with the aqueous environment and with proteins if the interaction of peripheral membrane proteins with the lipids is the subject of study. In such studies, monolayers possess an advantage over vesicular model systems in that their lateral density can be controlled and the effects of the lateral organization of the membrane model on protein adsorption processes may thus be determined [21]. On the other hand, since surface monolayers incorporate only on the order of 10^{14} molecules per cm^2 and only one planar surface is available for characterization, their description at the molecular level is much more difficult than that of vesicular systems and has been a major challenge in recent years that has furthered the development of surface specific, ultra-sensitive characterization methods. Still as of yet, this description has been mostly limited to layer models ('box models'), in which the lipid headgroups were modeled as one homogeneous slab with no discrimination of their molecular contents. Until recently, the reason for this has been the relative narrow range of momentum transfer available in reflectivity measurements, ~ 0.5 Å^{-1} with X-rays and ~ 0.25 Å^{-1} with neutrons (on D_2O), which corresponds to a resolution of 6 Å and >10 Å, respectively. With the advent of the latest generation of Synchrotron X-ray sources through the development of beam undulators, the available momentum transfer range has been significantly enlarged. It has thus become possible, and as we will show also necessary, to extend the classical box models and develop modeling strategies that go beyond.

Our efforts to develop a more elaborate quasimolecular description of lipid surface monolayers were motivated by an earlier study of protein adsorption to such systems [22]. In order to characterize the crystallization of bacterial S(*urface*)-layer proteins to dipalmitoylphosphatidylethanolamine we have measured the X-ray reflectivity of such systems up to large momentum transfer (maximum value, $q_z^{max} \sim 0.8$ Å^{-1}) and found that the structure of the lipid monolayer prior to protein adsorption could not satisfactorily be described in conventional slab models. Generally, such models work rather well with condensed monolayers at $q_z \leq 0.5$ Å^{-1} [23]; however, at higher q_z, discrepancies between the experimental data and the best-fit slab models are frequently observed.

In this paper, we examine a novel modeling strategy that describes phospholipid surface monolayers using a slab containing the hydrophobic chains, as in the classical two-box model, and distribution functions accounting for molecular fragments of the lipid headgroups whose positions may vary between individual lipid molecules. In this model, applied here to monolayers of the simple phospholipid dimyristoylphosphatidic acid (DMPA), the relative positions of the fragments have not been fixed, such that the phosphate may be located underneath, next to, or above the glycerol moiety. The spread of lipid headgroup conformations adopted within the monolayers as a function, e.g., of lateral pressure, pH or counterions is described by Gaussian functions that may vary in their center positions and half widths along the surface normal. This leads to a submolecularly resolved picture of the phospholipid monolayers on various subphases.

2. Materials and methods

2.1. Materials

DMPA, Na^+ salt, from Sigma (München, Germany) was used as supplied. Water was filtered using a Millipore (Bedford, MA, USA) Milli-Q system, yielding a residual specific resistance of better than 18.2 MΩcm.

2.2. Experimental

The X-ray instrument, located at the undulator beamline BW1 [24] of the DORIS III bypass at HASYLAB, Hamburg, Germany, is routinely used for

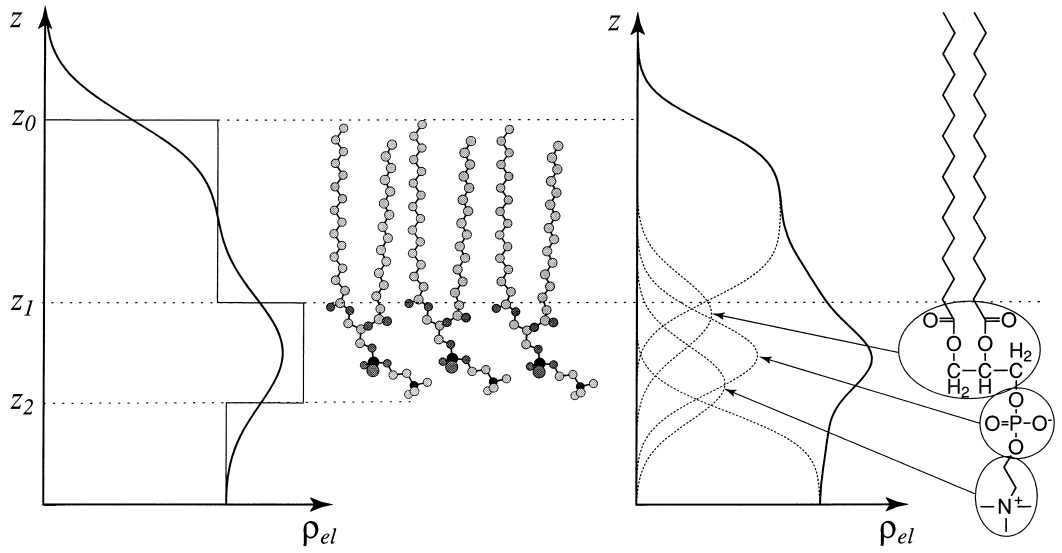

Fig. 1. Molecular depiction of lipid molecules in a Langmuir monolayer on an aqueous subphase (center) and parameterization of its structure in a conventional layer model ('box model', left) or in the quasimolecular description developed in this work (right). Shown as an example is DPPC. On the DMPA molecules investigated in this study, the terminal choline group is substituted by a hydrogen.

both reflection and GIXD measurements and has been described in detail earlier [25]. It allows reflectivity measurements down to $R \sim 5 \times 10^{-10}$. Briefly, a highly collimated monochromatic ($\lambda \sim 1.3$ Å) beam is directed at a shallow angle ($\alpha_{in} = 0... \sim 7°$) toward a water surface contained within the sealed container enclosing a Langmuir film balance. Before hitting the surface, the beam traverses two horizontally aligned entrance slits and optionally an calibrated Aluminum absorber. After reflection from the aqueous subphase that supports the organic monolayer, it is collected by a second pair of slits which reduce largely the background of incoherent scattering from the subphase. A NaI detector determines the signal, either after scattering of the reflected beam from a Kapton film ($q_z < 0.1$ Å^{-1}) to avoid detector overload or by receiving the reflected beam directly ($q_z > 0.1$ Å^{-1}). The instrument is automated and controlled by a work station.

We found that beam damage of the surface monolayer is an important issue in the full beam, particularly for phospholipid monolayers in the fluid phase. The monolayer was thus continuously shifted underneath the beam footprint to ensure that data are collected from undamaged areas within the surface film. Reproducibility of the measured data was checked routinely along various fragments of the reflectivity curve.

2.3. Quasimolecular models and data evaluation

2.3.1. General considerations

The structure of molecular lipid surface monolayers on aqueous subphases along the interface normal, z, has traditionally been modeled in two layers containing the hydrophobic tails and the hydrophilic headgroups of the molecules in which the lower one includes water that hydrates the headgroups. These layers are usually represented by 'boxes', i.e. step functions $\Theta(z-z_i)$ that describe changes of the scattering length density (SLD) $\rho(z)$ between the different molecular compartments that extend between z_0, the air/alkane interface, z_1, the interface between the hydrophobic and hydrophilic lipid slabs, and z_2, located at the boundary between the hydrophilic lipid slab and the water subphase (Fig. 1, left) [12,23]. In order to account for thermally excited capillary waves that broaden the entire molecular structure projected onto the z direction, the step functions are convoluted with a Gaussian, yielding the error function, $\frac{1}{2}\mathrm{erf}\left(\frac{z-z_i}{\sqrt{2}\sigma}\right)+\frac{1}{2}$, where $\mathrm{erf}(z) = 2/\sqrt{\pi}\int_0^z e^{-t^2} dt$ [6]. Due to the decrease of the surface tension γ upon decreasing molecular areas, A,

$$\gamma(A) = \gamma_0 - \pi(A), \quad (1)$$

(where γ_0 is the surface tension of the aqueous surface without lipid film and the lateral pressure π is monotonously rising upon decreasing A), the amplitude of the capillary waves, and thus the roughness parameter σ, rises slightly with increasing π/decreasing A [26].

For a data evaluation strategy that leads to a better description of the experimental data, we have parsed the lipid molecules into smaller components than in the conventional two-layer approach (Fig. 1, right). The number of molecular fragments and the parsing points within the molecule are constrained by the quality of the data, and it is obviously mandatory to keep the number of adjustable parameters at a minimum. The structure of the hydrophobic lipid acyl chains in surface monolayers has been extensively investigated using GIXD [6], and from these results, it seems most appropriate to treat the alkane fragments of the phospholipid as one molecular component in the model. We describe their distribution normal to the interface as a box function broadened into error functions with a global roughness parameter σ_{cw}, due to the capillary waves, just as in the two-layer approach. On the other hand, the lipid headgroups are both oversimplified and at the same time poorly understood in the conventional model. In the novel approach, we discriminate thus between several headgroup fragments. For the simple DMPA molecules described in this paper, the headgroups are simply parsed into the glycerol/carbonyl backbone ('GC') and the phosphate ('P') fragments. More complex lipids, such as phosphatidylcholine, may be described with a larger number of fragments. These fragments have a hydration shell of n_{GC}^{W} or n_{P}^{W} water molecules associated with them, that contribute to the SLD of the lipid headgroup components. Conceptually, we describe these locations by Gaussian distribution functions along z, similar to the model used for the description of lipid organization in oriented multi-bilayers by Wiener and White [27]. The interface between the composite headgroup and the underlying aqueous subphase is again described as an error function with the global roughness parameter, σ_{cw}.

This approach to data interpretation, for which the term 'composition–space refinement' has been coined by Wiener and White [27], possesses a number of obvious advantages, provided the quality of the experimental data permits the determination of a reasonably large number of model parameters. (a) The parameterization in terms of a quasimolecular structure enables the evaluation of either X-ray or neutron scattering data, or both in reference to one another. Since X-ray and neutron scattering lengths are independent of each other, the available information on the system effectively doubles if both types of data sets are refined with this method under the assumption that the underlying structure is independent of the scattering method used to characterize it. (b) The approach can be readily extended to more complex lipid headgroups or molecular compounds, such as peptides, interacting with the lipid headgroups. (c) The various quasimolecular components in this model may interpenetrate one another, such that the (average) orientation between the fragments may be evaluated. (d) The hydration of various fragments within the headgroup may be evaluated independent of each other. (e) While it is generally possible to determine the partial volumes of the molecular fragments from the fitting to the data [12], volumetric information obtained from other sources, e.g. from molecular dynamics simulations [28], may be used to constrain possible solutions that describe the experimental data to those that are space filling. In a recent paper, it has been shown [29] that such volume constrains may greatly enhance the information extracted from the analysis of the structure of lipid bilayer volume phases.

2.3.2. Application to DMPA monolayers

For an initial study of phospholipid monolayers, we have investigated the simple compound DMPA. In order to set up a quasimolecular model, the molecule has been parsed into just three components: the alkane, the GC and the P fragments. In practical terms, the contributions of the headgroup fragments to the SLD are treated as narrow boxes ($\Delta z = 1.5$ Å) with (unphysically large) SLD values, ρ_{box}, such that

$$b = \int_{z_k-\Delta z/2}^{z_k+\Delta z/2} \rho(z)\mathrm{d}z = \rho_{box}\cdot\Delta z \qquad (2)$$

accounts for the total scattering length, i.e. the number of electrons located on the fragment, including hydration water, with its center position at z_k. Between these boxes, the (unbroadened) SLD drops to

zero. Subsequent broadening into a sequence of error functions with a roughness parameter $\sigma_{erf} = \sigma_{total}$, results in a continuous SLD profile[1]. σ_{total} contains contributions of a global broadening, σ_{cw}, and an intrinsic broadening, σ_{int}, due to a distribution of the center of gravity of the molecular fragment along z:

$$\sigma_{total} = \sqrt{\sigma_{cw}^2 + \sigma_{int}^2} \quad (3)^2$$

This implementation permits the computation of the model reflectivity using the well-established and efficient Parratt formalism [30]. Since $2\sigma_{erf} \gg \Delta z$, the procedure leads to fragment distributions which are virtually indistinguishable from genuine Gaussian distribution functions. For $\Delta z \rightarrow 0$, the two functions are identical and $\sigma_{erf} = \sigma_{Gauss} \equiv \sigma$, since the convolution is applied to a δ function.

In initial runs of the modeling algorithm on the available data, we found that hydration of the GC group is negligible with respect to the sensitivity of the method. The best-fit models would suggest that typically less than 0.5 water molecule is bound to this molecular fragment. This is reasonable in view of the expectation that the phosphate group should contain much more water than the glycerol/carbonyl groups and is consistent with experimental findings [15] and simulations [29,31] concerning phospholipid bilayers. We have consequently neglected GC hydration in the discussion of the monolayer structure. In order to simplify the quasimolecular model further, we have used the fact that the GC fragment is directly attached to the alkane chains and possesses a restricted conformational flexibility. We have thus coupled the position of the GC fragment to the chain end, locking the center of gravity of the group at a distance

$$\Delta z_{GC-chain\ end} = 0.5 \cdot \frac{V_{GC}}{A_{lipid}} \quad (4)$$

to the chain ends, where V_{GC} is the partial molecular volume of the GC fragment and A_{lipid} is the area per DMPA molecule within the monolayer as determined from the isotherm.

As a constraint to the electron density distributions used to fit the experimental data, space filling was optimized for the hydrophilic sections of the monolayer. Following Petrache et al. [28], we have defined probabilities $p_\xi(z)$ to find a contribution of the component species ξ (where ξ indicates GC, P or subphase water; hydration water is accounted for within the contributions of P and, in principle, GC) at a vertical distance z from the hydrophobic chain/air interface with

$$\sum_\xi p_\xi(z) = 1 \quad (5)$$

If $n_\xi(z)$ denotes the number density, as determined from the model, and V_ξ the partial volume of the component ξ, then

$$\sum_\xi n_\xi(z) \cdot V_\xi = 1 \quad (6)$$

is the condition for homogeneous filling of the available space at a depth z within the monolayer. In the model refinement, we have evaluated $N = 40$ horizontal slabs with a width of $\Delta z = 1$ Å between $z = -10$ Å and -50 Å to find the variance

$$X = \frac{1}{N}\sum_{i=1}^{N}\left(\sum_\xi n_\xi(z_i) V_\xi - 1\right)^2 \quad (7)$$

as a quantitative measure of the deviation of a particular model from homogeneous space filling. This quantity has been added to the χ^2 value, as determined in the usual way from the quadratic sum of the deviations, normalized to the experimental error bars, of the model reflectivity from the experimental values, to arrive at

$$\chi'^2 = \chi^2 + e^{D\chi} \quad (8)$$

where D is a weighting factor for the volume constraint; we chose a value $D = 800$ for the evaluation of the data reported in Section 3. χ'^2 was then used as the criterion to quantify the quality of the model. Starting values for the partial molecular volumes of the GC and P fragments have been taken from molecular simulations of phosphatidylcholine (DPPC,

[1] This procedure is justified because the contrast in the SLDs of the spatially distributed molecular fragments in typical Langmuir monolayers is low.

[2] The geometric summation is motivated by the expectation that the lateral length scales of capillary waves and the molecular roughness within the monolayer are quite different [26].

DOPC and POPC) bilayer systems [29], $V_{GC} = 146.8$ Å^3 and $V_P = 53.7$ Å^3. For the component volume of water, the bulk value $V_W = 30.0$ Å^3 has been used. Although data have been routinely collected from $q_z \sim 0.01$ Å^{-1} upwards, only those data points with $q_z > 0.1$ Å^{-1} have been used in the refinement, since the experimental error bars, determined exclusively from counting statistics, are exceedingly small for low q_z such that minute systematic errors would bias the models strongly, possibly overriding information contained at high q_z values.

3. Results

3.1. General assessment of the new approach to data refinement

Fig. 2 shows various model fits in comparison with the experimental data for a DMPA monolayer on pure water at $\pi = 45$ mN/m. To visualize even small discrepancies between the models, the reflectivities are displayed normalized to the Fresnel reflectivity, R_F, of the pure subphase. To enable a direct comparison with the composition–space refinement approach developed in Section 2, A_{lipid} from the isotherm and volumetric information has been used to keep the number of adjustable parameters low. It is quite obvious that a conventional two-slab model with one surface roughness parameter that accounts for capillary waves at the interface is entirely incapable of describing the experimental data above $q_z \sim 0.5$ Å^{-1} (dashed line). Similarly, a two-slab model with three different roughness parameters predicts reflectivities that describe the experimental data only poorly, particularly at high q_z (dotted line). Note that even if the correspondence between the model reflectivity and the data is improved in the latter approach, there is no straightforward chemical interpretation for such a model. In quantitative terms, the χ^2 values are 7.8 and 1.9 for the two-slab models with one or three roughness parameters, i.e. three or five adjusted parameters, respectively. If one uses a three-box model with one roughness parameter (four adjustable parameters), the χ^2 is even larger within the constraints of chemical plausibility (no negative number of water molecules within any headgroup box) than that obtained with the two-box model. This procedure is incapable of placing the phosphate fragment in a reasonable context with the GC fragment, since both molecular components are not allowed to interpenetrate each other. Finally, if one uses box models without any chemistry-related constraint, adjusting widths and SLDs freely, one finds a $\chi^2 = 2.4$ for the data set shown in Fig. 2 for a two-box model with one roughness parameter (five adjustable parameters). One has to conclude that, particularly at large q_z, box models are not well-suited to describe the reflectivity data set.

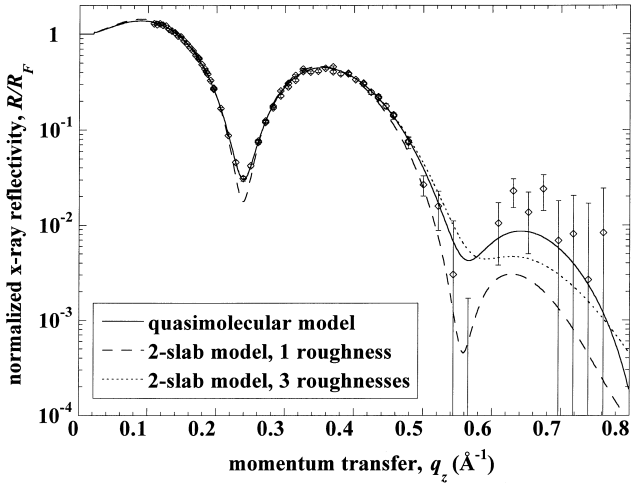

Fig. 2. Comparison of the best-fit descriptions, afforded by various models as indicated, of the X-ray reflectivity R, normalized by the Fresnel reflectivity R_F, for a DMPA monolayer on water at $\pi = 45$ mN/m and $T \sim 27$°C.

Also shown in Fig. 2 as a solid line is a model reflectivity from the quasimolecular composition–space refinement approach described above. Since the model has been stripped to its bare bones, only five adjustable parameters have been determined from the refinement: the thickness of the alkane slab, d_{chain}, the center position of the phosphate fragment, z_P, the global (capillary waves) and the intrinsic roughness parameters, σ_{cw} and σ_{int}, and the number of water molecules associated with the phosphate fragment, n_P^W. The area per DMPA molecule within the monolayer, $A_{lipid} = 42$ Å^2, has been taken from the isotherm and the component volumes, $V_{GC} = 146.8$ Å^3 and $V_P = 53.7$ Å^3, have been taken from the literature [29]. Note that even better fits to the data can be achieved within this model if one releases the constraint of space filling. With this con-

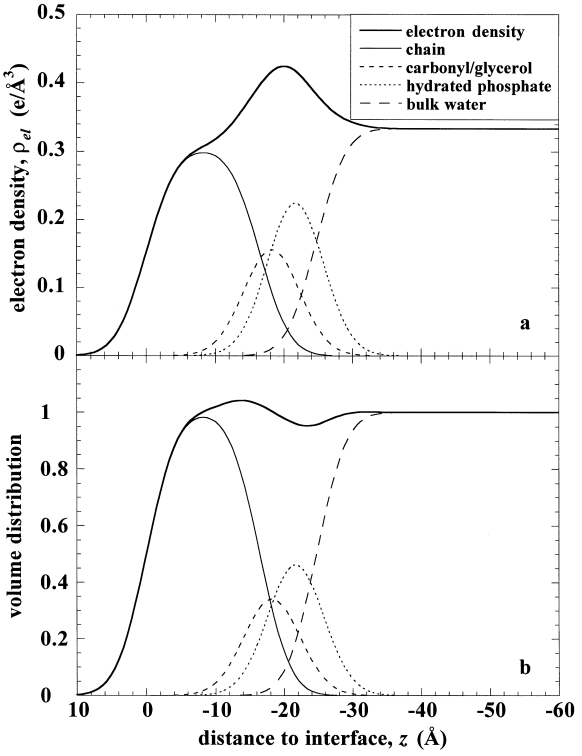

Fig. 3. (a) Electron density distribution and (b) volume distribution in a DMPA monolayer ($\pi = 45$ mN/m, $T \sim 27$°C) on a water subphase as derived from the quasimolecular modeling of the experimental data shown in Fig. 2.

straint enforced, $\chi^2 \sim 1.8$, while the variation of space filling amounts to $X \sim 5 \times 10^{-4}$, such that $\chi'^2 \sim 3.3$. In this model, the chain slab has a thickness $d_{chain} \sim 16.5$ Å, the center position of the GC component is located at $z_{GC} \sim 18.3$ Å and that of the P component at $z_P \sim 21.7$ Å. Slightly less than five water molecules hydrate the latter fragment of the lipid molecule. The broadening of the interface structure due to capillary waves is $\sigma_{cw} \sim 3.5$ Å and the additional intrinsic broadening due to a distribution of the headgroup components along the z axis is $\sigma_{int} \sim 2.15$ Å, such that the width of the Gaussian distributions amounts to $\sigma_{Gauss} \sim 4.1$ Å, c.f. Eq. 3. Fig. 3 shows the electron density distribution and the volume distribution across the interface and gives the contributions of the various components. It is obvious that the space filling is not quite homogeneous with a few percent overfilling in the interface region between the alkane chains and the GC fragment while underfilling occurs around the position of the P fragment.

In order to estimate confidence limits of the determined quantities, one may map χ'^2 in parameter space by arbitrarily fixing a selected parameter while readjusting all others to find a new local minimum of χ'^2 [12]. Such maps are shown in Fig. 4 for the four parameters that describe the molecular structure of the phospholipid: d_{chain}, z_P, n_P^W and σ_{int}. The fifth adjusted parameter, not shown in Fig. 4, is $\sigma_{cw} = 3.5 \pm 0.06$ Å, which describes a collective property of the surface. If one arbitrarily chooses to define the limits of confidence at those parameter values where χ'^2 is increased by 10% over its global minimum, one reads from Fig. 4: $d_{chain} = 16.5 \pm 0.15$ Å, $z_P = 21.7+0.4/-0.8$ Å, $n_P^W = 4.8+1.2/-2.5$ and $\sigma_{int} = 2.15 \pm 0.2$ Å. In a similar vein, one may check the assumptions on the constants A_{lipid}, V_{GC} and V_P by varying their values and readjusting the structural parameters. We deduce that the assumptions are reasonable, since all values are found within the confidence limits determined by the mapping procedure: $A_{lipid} \sim 43$ Å^2, $V_{GC} \sim 155$ Å^3 and $V_P \sim 60$ Å^3 would slightly improve the best-fits as observed with the constants taken from the isotherm or from the molecular simulation work [29]. Particularly for the component volumes, the observed minima are so shallow, however, that well-defined values which might better describe the situation in the monolayer cannot be determined from the data.

3.2. The structure of DMPA in monolayers on pure water subphase

Fig. 5 shows the isotherm ($T = 26.8 \pm 0.5$°C) of DMPA on pure water and indicates where reflectivity measurements have been taken to evaluate the structure of the molecules within the surface monolayer. The isotherm shows the well-known [32] first-order phase transition between the liquid-expanded, LE[3], and the liquid-condensed, LC[3], phases at $\pi \sim 8$ mN/m. While we have measured the structure of the monolayer in the LE phase at $\pi = 2$ mN/m and at 4 mN/m, and in LC at 15 mN/m and 30 mN/m, respectively, we have deliberately omitted the phase coexistence region, since it is well-established [34,35] that this region is characterized by macroscopic

[3] Phases are denoted according to Cadenhead et al. [33].

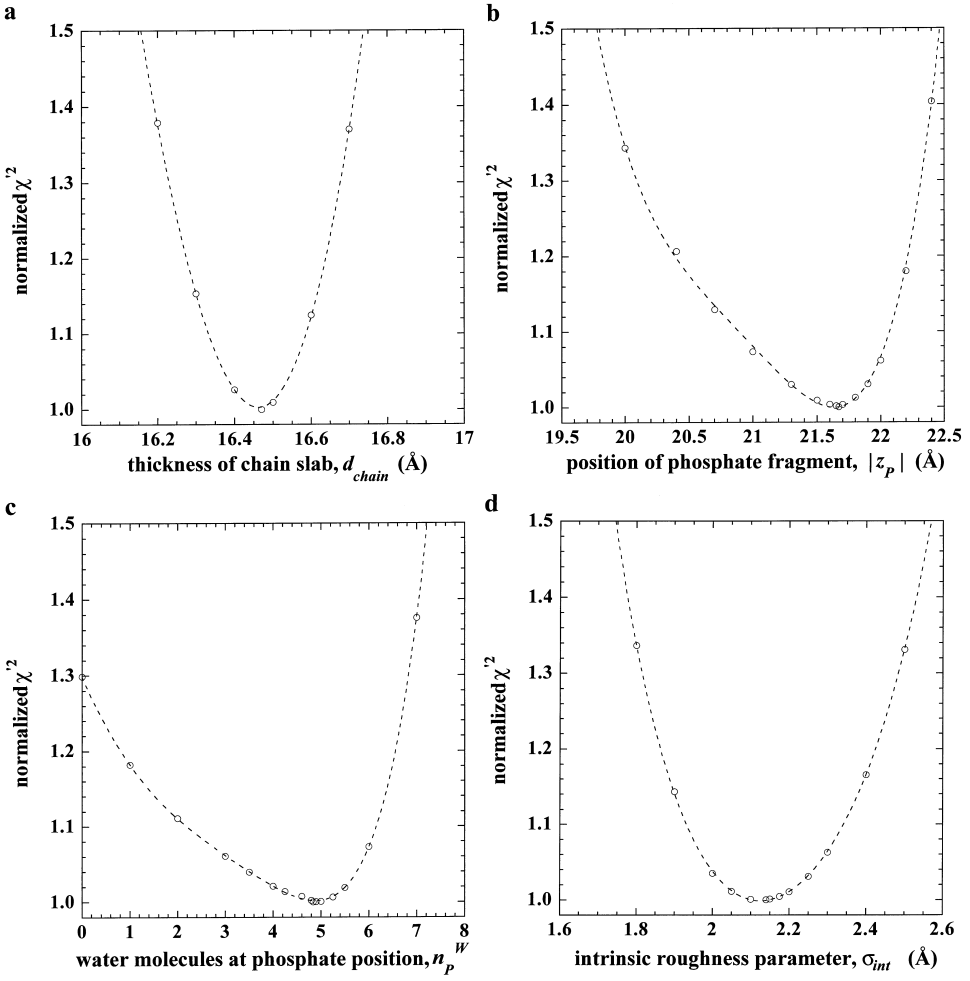

Fig. 4. Results from the χ'^2 mapping of fits obtained from the quasimolecular modeling of the DMPA monolayer data ($\pi = 45$ mN/m, $T \sim 27$°C) shown in Fig. 2 as described in detail in the text. For the determination of confidence levels on the model parameters, an increase of the χ'^2 value of 10% above its minimum has been permitted. Dotted lines are guides for the eye.

phase separation, such that the number of parameters determining the microscopic structure there is essentially doubled. At $\pi \sim 40$ mN/m, a further phase transition to a solid-condensed, SC^3, phase occurs [36]. We have thus also measured the reflectivity at 45 mN/m. In all cases, we observed that the quasimolecular model yields a better agreement between the models and the experimental data than the two-slab models, although in the LE phase ($\pi = 2$ mN/m and 4 mN/m), the qualities of the fits are comparable. The experimental data sets together with the reflectivities of the optimized quasimolecular models are shown in Fig. 6.

In Table 1, the results from the data evaluation are summarized. It is obvious that the conformational properties of the alkane chains dictate the behavior of the entire molecule. This is also visualized in Fig. 7 which displays some of the results contained in Table 1. If one compares the extended length values of the chains and the headgroup ($l_{\mathrm{chain}} = 16.7$ Å and $l_{\mathrm{head}} = 5.3$ Å[4]) with the obtained distances between the molecular fragments projected on the z axis, one may estimate average tilt angles of the chains and headgroups, β and α, from the surface normal. Fig. 7a thus shows the variation of the chain tilt angle β as a function of the lateral pressure π as it follows from the thickness d_{chain} of the slab that contains the

[4] l_{head} has been evaluated as the distance from the phosphorous position to the center of mass of the GC fragment in an MM2-optimized model of the DMPA molecule.

hydrophobic chains. The general behavior is similar to that observed for DMPE in earlier work, where the structure has been interpreted in a two-slab approach [23]. Across the LE→LC phase transition, the slope $d(d_{chain})/d\pi$ decreases by an order of magnitude. More interesting and more subtle, however, is the development of the headgroup conformation along the isotherm. Fig. 7b indicates that the headgroup orientation follows the changes of the acyl chain conformations closely. This is reflected in the behavior of the average headgroup tilt angle which is large, $\alpha \sim 65°$, in the LE phase and decreases significantly, to $\alpha \sim 48°$, in the LC and SC phases. Concomitantly with the squeezing out of the headgroup from the plane of the monolayer, we observe a continuous increase of the distribution width σ_{int} as π rises beyond 30 mN/m (Fig. 7c). At first sight, σ_{int} seems to follow σ_{cw}, the global roughening of the interface which increases with π as the amplitude of the capillary waves rises. We note, however, that the two quantities are not interrelated such that the increase of σ_{int} is probably of different origin.

The development of the phosphate hydration upon compression of the monolayer, finally, reflects both the discontinuous decrease of the molecular area A_{lipid} and the tilting of the lipid headgroups toward the surface normal, i.e. the reduction in α. If headgroup hydration was entirely determined by the available area within the film, n_P^W should be expected to drop by almost a factor of two between $A_{lipid} = 70$ Å^2 and 42 Å^2. Tilting of the headgroup toward the surface normal together with the high affinity of the phosphate group to water leads to a much smaller effect, such that the volume occupied by water within the headgroup is almost constant across the whole isotherm (Fig. 7d).

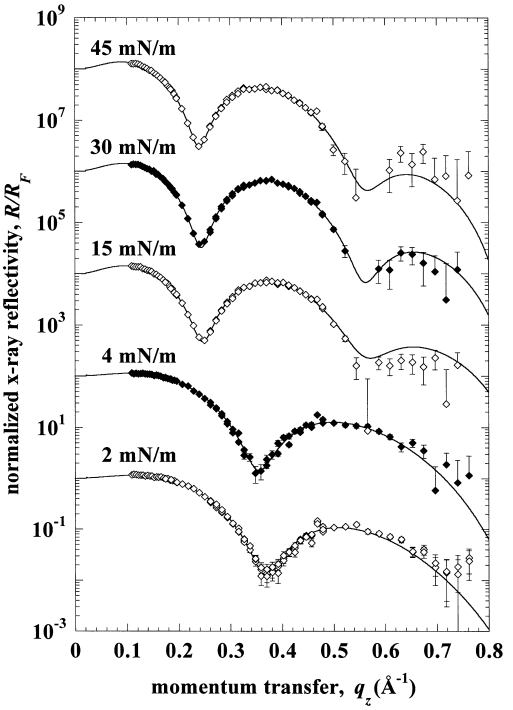

Fig. 6. Normalized X-ray reflectivity, R/R_F, of DMPA at $T = 26.8 \pm 0.5$°C as a function of lateral pressure π, and best-fits to the experimental data derived from quasimolecular modeling (lines). Error bars have been determined from counting statistics. Data for $q_z < 0.1$ Å^{-1} are not shown. For clarity, data corresponding to $\pi > 2$ mN/m have been multiplied by multiples of 100. Also, some of the negative error bars at high q_z have been omitted for clarity.

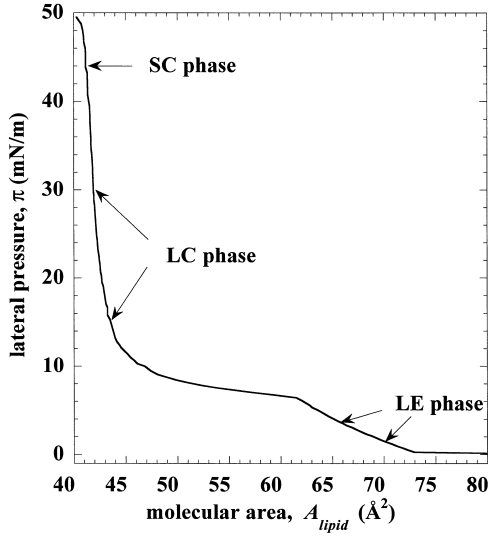

Fig. 5. Isotherm of DMPA on water at $T = 26.8 \pm 0.5$°C. Indicated are the locations where X-ray reflectivity measurements have been obtained.

4. Discussion

Submolecular resolution of the structure of lipid surface monolayers is not a trivial issue, both in terms of the scientific questions that may be tackled and in terms of technical realization. Our long-term goal in this field aims at elucidating the interactions of adsorbent molecules with membrane interfaces. As an example, we have recently investigated the

Table 1
Structural parameters describing DMPA molecules in a Langmuir monolayer on pure water as derived from composition–space refinement of X-ray reflectivity data

Lateral pressure	π (mN/m)	2	4	15	30	45	
Area per molecule	A_{lipid} (Å^2)	70	67	44	43	42	Constant
Chain slab thickness	d_{chain} (Å)	10.6 ± 0.2	11.3	15.5	15.9 ± 0.12	16.5 ± 0.15	Parameter
Average chain tilt angle	β (°)	51	47	22	18	9	Dependent variable
GC position	z_{GC} (Å)	−11.7	−12.4	−17.2	−17.6	−18.3	Dependent variable
P position	z_{P} (Å)	$-13.9^{-1}_{+0.7}$	−14.75	−20.7	$-21.2^{-0.5}_{+0.3}$	$-21.7^{-0.8}_{+0.4}$	Parameter
Projected GC–P distance	$d_{\mathrm{GC-P}}$ (Å)	2.3	2.35	3.5	3.6	3.5	Dependent variable
Average headgroup orientation angle	α (°)	65	63	48	47	48	Dependent variable
Global interface distribution width	σ_{cw} (Å)	3.1 ± 0.1	3.0	2.9	3.1 ± 0.1	3.5 ± 0.1	Parameter
Internal fragment roughness	σ_{int} (Å)	1.4 ± 0.3	1.7	1.8	1.9 ± 0.2	2.2 ± 0.2	Parameter
Total width of distribution function	σ_{total} (Å)	3.4	3.4	3.4	3.6	4.1	Dependent variable
Water molecules per headgroup	$n_{\mathrm{P}}^{\mathrm{W}}$	$6.2^{+3.5}_{-5}$	6.5	4.7	5.0^{+1}_{-2}	$4.8^{+1.2}_{-2.5}$	Parameter

For the component volume values from molecular simulations [29], $V_{\mathrm{GC}} = 146.8$ Å^3 and $V_{\mathrm{P}} = 53.7$ Å^3, have been assumed. The extended lengths of the myristoyl chains, $l_{\mathrm{chain}} = 16.7$ Å, and the distance between the center of gravity of the GC fragment and the phosphate in an extended configuration, $l_{\mathrm{GC-P}} = 5.27$ Å, have been estimated from a MM2-optimized molecular model. Confidence limits on the adjustable model parameters have been estimated by mapping χ'^2 in parameter space (see text) in which a 10% increase over the minimum of χ'^2 has been used as the criterion. For $\pi = 4$ mN/m and 15 mN/m, confidence limits have not been determined. Dependent variables have been computed using a higher numerical precision of the independent parameters than the one shown.

adsorption and recrystallization of bacterial S-layer proteins at phospholipid surface monolayers [22,37, 38]. We observe subtle changes in the electron density of the lipid headgroup region which became only obvious when we analyzed the reflectivity from the compound layer system at large q_z. In the line of that work, we found that the X-ray reflectivity of simple lipid monolayers cannot be satisfactorily described within the conventional slab model approach [22]. Specifically, data refinement with a model-free approach [39] suggested that the interface between the chain slab and the headgroup slab is more broadened than would be expected from the thermal excitation of capillary waves. In addition, we observed an increase in electron density underneath the headgroup slab which may in that case be attributed to a cloud of adsorbed ions. The important point, however, is that, while we were able to quantify changes in the electron density of the lipid headgroups, we were incapable of interpreting these changes in molecular terms. Hence it appeared that the molecular structure of pure lipid monolayer systems had to be revisited.

The work reported here concerns a first approach to more detailed models of phospholipid headgroups in surface monolayers by analyzing the simplest case: the structure of DMPA. From there it is obvious to extend such investigations to systems that are more sophisticated, charged lipids with bound counterions or more complex lipid molecules. Eventually, we foresee a possibility to analyze in molecular detail subtle changes in the lipid headgroup structure upon adsorption and/or intercalation of (macro)molecules from the adjacent aqueous phase, surfactants, peptides, proteins, polysaccharides or nucleic acids. To that end, it is quite likely that X-ray reflectivity measurements will contribute only one, however important, piece of information that is to be supplemented with complementary techniques, such as neutron reflectometry, GIXD, FTIR spectroscopy and molecular modeling.

For DMPA in surface monolayers on pure water, it is quite obvious that the quasimolecular approach that we have introduced describes the experimental data much better than the conventional slab models,

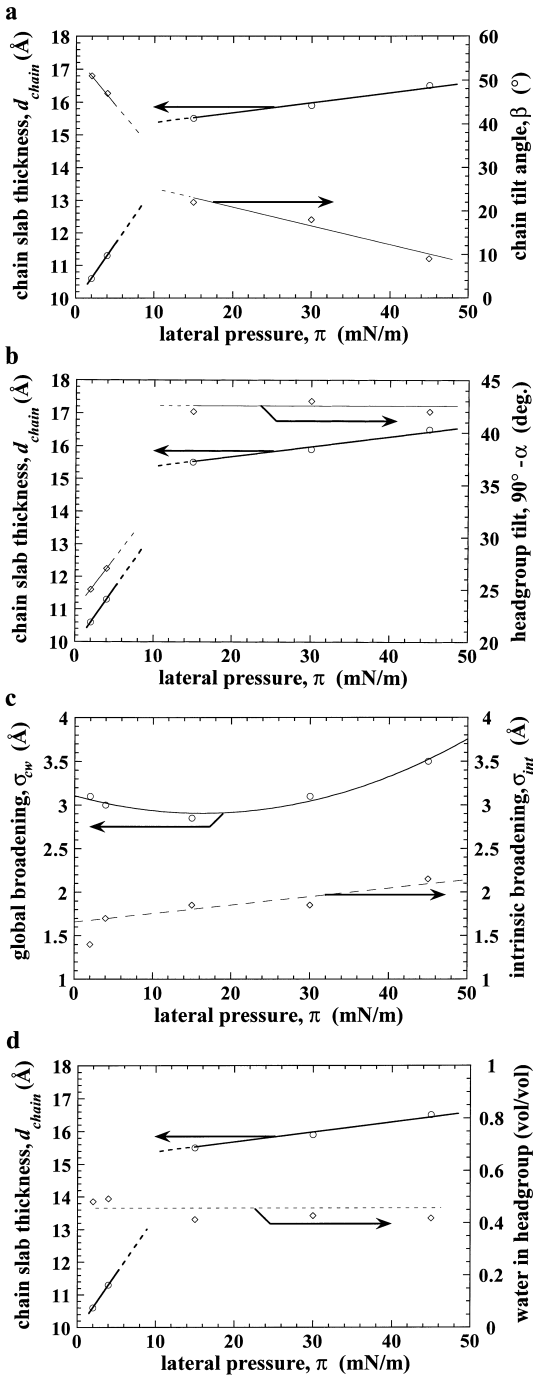

Fig. 7. Pressure-dependence of various parameters describing the structure of a DMPA monolayer on water as derived from quasimolecular modeling of X-ray reflectivity measurements. Between 7 and 10 mN/m, the main monolayer phase transition (LE→LC) occurs, c.f. Fig. 5. Lines in the plots are guides for the eye. For details, see text.

c.f. Fig. 2. While the simple two-slab model is certainly incapable of reproducing the experimental data at high q_z, more sophisticated slab models lack a straightforward chemical interpretation and are thus inept of quantifying structural changes in the molecules in more complex problems. Moreover, the relative deficiency of the conventional slab models is even more pronounced for phospholipids of higher complexity, such as phosphatidylcholine or phosphatidylglycerol (Krüger et al., manuscript in preparation). On the contrary, the novel approach we have taken here accomplishes modeling the experimental data with a minimum of adjusted parameters. It constitutes a description capable of representing the lipid headgroups in their full conformational flexibility and seems thus well-suited to further the description of such systems. In the course of its evaluation, the availability of volumetric information from molecular modeling [28,29] greatly facilitated the determination of structural parameters from the experimental data.

The following picture emerges for the structure of DMPA on pure water. The ordering of the acyl chains governs the lipid's phase behavior. At the main, LE→LC, phase transition, the average tilt angle β decreases from $\sim$45° to $\sim$20° and further on to $\sim$10° in the SC phase, see Fig. 7a. This is, of course, an old result, and it has been shown in pioneering GIXD work that hexatic ordering of the chains is inferred by the LE→LC transition [36]. Positionally correlated ordering of the chains, however, was only observed in the SC phase [36]. No information has been revealed from this type of work about the phospholipid headgroups. These are either too low in their electron density or too disordered to contribute measurably to the diffraction, or both. In contrast to the situation concerning lipid multi-bilayer systems [14,15,29,40], no direct information, to our knowledge, has been extracted to date on the orientation of headgroup fragments of phospholipids in surface monolayers.

From the work reported here, we conclude that the DMPA headgroup follows the organizational changes of the chains closely, c.f. Fig. 7b. In the LE phase, the average orientation of the headgroups, as determined from the projected distance between the GC and P fragments, is close to the plane of the interface, $(90°-\alpha)\sim 25°$. Reduction of the avail-

able area, A_{lipid}, in the course of the main phase transition to LC causes a tilting movement of the headgroups away from the interface to $\alpha \sim 45°$. Further compression of the monolayer into the SC phase does not measurably affect the lipid headgroups. Only a continuous increase of the intrinsic spread of the projected phosphate positions around their mean value is observed, suggesting that the headgroups respond to the increase in positional ordering of the chains with conformational rearrangements that do not affect the average tilt angle from the interface.

The roughness parameters σ_{cw} and σ_{int} which have to be distinguished in the quasimolecular model are of different physical origin and show thus a different development upon changes in the lateral pressure, c.f. Fig. 7c. As also observed in the conventional two-slab evaluation of data [13], σ_{cw} decreases at first slightly with increasing π since the molecular roughness of the alkane phase toward the air compartment decreases, and this contribution to the interface roughness is effectively contained in the parameter σ_{cw}. As the alkane/air interface roughness is essentially constant in the LC and SC phases, σ_{cw} is expected to increase more than linearly following the increasing amplitude of the capillary waves. This is observed in the model. In comparison, the intrinsic molecular roughness of the headgroup fragments, σ_{int}, increases only slightly along the isotherm and does so rather linearly as suggested by a fit to the data[5] which is shown in Fig. 7c just as a guide for the eye. The important point to note here, however, is that the headgroup fragment distribution is definitively larger than broadening exclusively by capillary waves would suggest, owing to the conformational flexibility of the headgroup. This is an essential feature of the novel modeling approach and is one of the reasons why this model is capable of describing the experimental data better than the slab models.

Surprising in view of older interpretations of phospholipid monolayer structure [1,13] is that the quasimolecular model suggests that headgroup hydration is essentially constant along the isotherm (see Table 1 and Fig. 7d). In a detailed evaluation of the (low q_z) X-ray reflectivity of diacyl-PE monolayers in the framework of a two-box model, it was concluded that the electron content of the headgroup (plus associated water) is largely different in the LE and LC phases and depends sensitively on the molecular area within each of the phases [13]. A straightforward interpretation of that observation is that water molecules are squeezed out of the lipid headgroups as the monolayer is compressed, from $n^{W}_{headgroup} \sim 24$ at $A_{lipid} \sim 80$ Å^2 to $n^{W}_{headgroup} = 14$ or 18 for DLPE or DMPE, respectively, at the onset of their phase transitions and eventually to $n^{W}_{headgroup} \sim 1.5$ in the SC phase of DMPE according to the two-box model. This change by an order of magnitude seems unrealistic, however, a careful examination by the authors of that study concluded with the statement that within the two-box approach, this result was robust against variations of details of the model [13]. Even if one bears in mind that the lipids used in the earlier study and in this study are different and may interact differently with water, it seems odd that the PE headgroup should bear so much more water molecules in the LE phase than does the PA group as revealed in this work. In our view, it seems quite likely that the remarkable change reported for the PE headgroup hydration is an artefact of the slab model approach. As the model is incapable of handling various headgroup fragments separately, the 'headgroup volume', evaluated as $V^{two-box\ model}_{headgroup} = A_{lipid} \cdot d_{headgroup}$ where $d_{headgroup}$ is the extension of the headgroup slab along the surface normal, is overestimated and water molecules that do not associate with the headgroup are counted. Fortunately, since the average orientation of the GC→P fragment, at least in DMPA, is in all situations closer to the surface plane than to the surface normal, the two-box model continues to work within its limitations as one goes from the LE phase to the LC and SC phases. Would the phosphate group be expelled from the hydrophobic/hydrophilic interface to an extent that $\alpha \sim 0$, the two-box model was bound to fail in describing the high pressure data. The observation that a volume-constrained three-box model describes the data even more poorly than the two-box model (see comparative evaluation of the different modeling strategies at the beginning of the Section 3) emphasizes this point and is consistent with our result that the GC→P

[5] In this fit, we have deliberately omitted the point at $\pi = 2$ mN/m, which may lie systematically low while due to the large alkane/air roughness all interfaces seem broadened, indistinguishable from a broadening by capillary waves.

fragment is oriented close to the interface. It has to be concluded that headgroup hydration and its development with lateral pressure are severely misinterpreted in the box approach.

In contrast to the published behavior of DMPE headgroup hydration in monolayer films, we observe an essentially constant hydration of the DMPA headgroup along the isotherm as shown in Fig. 7d. We regard this result reasonable in view of the strong hydrophilicity of the charged phosphate group and postulate that the headgroup rearrangements upon reduction of the available area A_{lipid} within the film can be accounted for if one takes into consideration that the phosphate is unlikely to abandon its strongly bound hydration shell. If similar results hold for zwitterionic lipids such as PE or PC remains to be seen. In any case, changes in hydration seem more plausible in such systems. In fact, for (chain-deuterated) DPPC, a pressure-dependent shift of the asymmetric PO_2^- stretch vibration near 1220 cm^{-1} observed in FTIR spectroscopy at the air/water interface has been interpreted as a dehydration effect [41].

As a final remark, we found occasionally slightly better fits to the data if the component volumes were varied around those values that derive from molecular simulation work [28,29] and were used in this study. Since the simulations were performed on hydrated bilayer models and may describe a slightly different situation than that of lipid monolayers at the air/water interface, one may ask whether the observed deviations are real such that modified fragment volumes ought to be used for reflectivity data refinement. While χ'^2 mapping suggested that the bilayer modeling results are consistent with the experimental results, it showed also that it is impossible at the current stage to determine better values from fitting to the available data. In any case, we observe that slight changes in A_{lipid}, V_{GC} and V_{P} do not change the gross picture that emerges from this work and just note that the combined use of X-ray and neutron data measured with equally prepared systems should conceivably improve on the situation.

5. Conclusions

For the phospholipid DMPA, we have shown that a refined model of the lipid headgroups, in which the spatial organization of submolecular fragments is accounted for by distribution functions across the interface, leads to a much more realistic description than box models and yields a detailed conception of the headgroup response to the main monolayer phase transition LE→LC. During the phase transition, which is accompanied with a large reduction of the area available to the molecules within the surface film, the headgroups tilt collectively toward the surface normal, from $\alpha \sim 65°$ to $\sim 48°$, while the spread of the orientation angle around its mean value is approximately constant (or increases continuously across the transition). Upon entering the positionally ordered SC phase at high π, no further rearrangement of the lipid headgroups has been revealed.

Particularly disparate are the interpretations of the lipid headgroup structure with respect to hydration that are derived from the quasimolecular model on the one side and slab models on the other. While it has been reported for PE in the LE phase that the hydration amounts to almost 20 water molecules per lipid and changes by an order of magnitude upon compression, we observe a low ($\sim$5–6) number of water molecules associated with the phosphate in DMPA throughout the isotherm. We have traced these differences to inherent deficiencies of the box model approach and conclude that this model is quite incapable of describing lipid headgroups realistically.

While this paper has been devoted to developing and establishing a more refined microscopic model of Langmuir monolayers from X-ray reflectometry, it is left to future work to extend these tools to more relevant systems. As a preeminent goal for the future, we foresee the quantitative characterization of phospholipid headgroup reorganization upon interaction of adsorbent molecules with membrane interfaces.

Acknowledgements

We thank Kristian Kjaer (Risø National Laboratory, Roskilde, Denmark) for his devising of the liquid surface experimental station at BW1 and valuable advice for the experimental work and Thomas Gutberlet (HMI Berlin) for his help with some of the measurements. We acknowledge beam time at

HASYLAB (DESY, Hamburg, Germany) under the BMBF contract 03-LO4LEI-8 and the HASYLAB project no. II-97-51. The work has been financially supported by the DFG through the SFB 294 (TP C10) and by the Fonds der Chemischen Industrie (Frankfurt, Germany).

References

[1] H. Möhwald, Annu. Rev. Phys. Chem. 41 (1990) 441.
[2] H.M. McConnell, Annu. Rev. Phys. Chem. 42 (1991) 171.
[3] C.M. Knobler, R.C. Desai, Annu. Rev. Phys. Chem. 43 (1992) 207.
[4] M. Lösche, E. Sackmann, H. Möhwald, Ber. Bunsenges. Phys. Chem. 87 (1983) 848.
[5] R.M. Weis, H.M. McConnell, Nature 310 (1984) 47.
[6] J. Als-Nielsen and H. Möhwald, in: S. Ebashi, M. Koch and E. Rubinstein (Eds.), Handbook on Synchrotron Radiation, Elsevier North-Holland, Amsterdam, 1991.
[7] J. Als-Nielsen, D. Jacquemain, K. Kjaer, M. Lahav, F. Leveiller, L. Leiserowitz, Phys. Rep. 246 (1994) 251.
[8] R. Mendelsohn, J.W. Brauner, A. Gericke, Annu. Rev. Phys. Chem. 46 (1995) 305.
[9] V.M. Kaganer, H. Möhwald, P. Dutta, Rev. Mod. Phys. 71 (1999) 779.
[10] J. Als-Nielsen and K. Kjaer, in: T. Riste and D. Sherrington (Eds.), Phase Transitions in Soft Condensed Matter, Plenum Press, New York, 1989, p. 113.
[11] J. Penfold, R.K. Thomas, J. Phys. Condens. Matter 2 (1990) 1369.
[12] D. Vaknin, K. Kjaer, J. Als-Nielsen, M. Lösche, Biophys. J. 59 (1991) 1325.
[13] C.A. Helm, P. Tippmann-Krayer, H. Möhwald, J. Als-Nielsen, K. Kjaer, Biophys. J. 60 (1991) 1457.
[14] G. Büldt, H.U. Gally, J. Seelig, G. Zaccai, J. Mol. Biol. 134 (1979) 673.
[15] M.C. Wiener, S.H. White, Biophys. J. 61 (1992) 434.
[16] D.A. Pink, S. McNeil, B. Quinn, M.J. Zuckermann, Biochim. Biophys. Acta 1368 (1998) 289.
[17] D.A. Pink, M. Belaya, V. Levadny, B. Quinn, Langmuir 13 (1997) 1701.
[18] S.E. Feller, R.M. Venable, R.W. Pastor, Langmuir 13 (1997) 6555.
[19] S.E. Feller, D. Yin, R.W. Pastor, A.D. MacKerell Jr., Biophys. J. 73 (1997) 2269.
[20] D. Huster, K. Arnold, K. Gawrisch, J. Phys. Chem. B103 (1999) 243.
[21] A. Diederich, C. Sponer, D. Pum, U.B. Sleytr, M. Lösche, Colloids Surf. B Biointerf. 6 (1996) 335.
[22] M. Weygand, B. Wetzer, D. Pum, U.B. Sleytr, K. Kjaer, P.B. Howes, M. Lösche, Biophys. J. 76 (1999) 458.
[23] C.A. Helm, H. Möhwald, K. Kjaer, J. Als-Nielsen, Europhys. Lett. 4 (1987) 697.
[24] R. Frahm, J. Weigelt, G. Meyer, G. Materlik, Rev. Sci. Instrum. 66 (1995) 1677.
[25] J. Majewski, R. Popovitz-Biro, W.G. Bouwman, K. Kjaer, J. Als-Nielsen, M. Lahav, L. Leiserowitz, Chem. Eur. J. 1 (1995) 304.
[26] P.S. Pershan, Faraday Discuss. Chem. Soc. 89 (1990) 231.
[27] M.C. Wiener, S.H. White, Biophys. J. 59 (1991) 174.
[28] H.I. Petrache, S.E. Feller, J.F. Nagle, Biophys. J. 70 (1997) 2237.
[29] R.S. Armen, O.D. Uitto, S.E. Feller, Biophys. J. 75 (1998) 734.
[30] L.G. Parratt, Phys. Rev. 95 (1954) 359.
[31] K.V. Damodaram, K.M. Merz Jr., Langmuir 9 (1993) 1179.
[32] O. Albrecht, H. Gruler, E. Sackmann, J. Phys. (Fr.) 39 (1978) 301.
[33] D.A. Cadenhead, F. Müller-Landau and B.M.J. Kellner, in: S.K. Sinha (Ed.), Ordering in Two Dimensions, Elsevier North Holland, Amsterdam, 1980, p. 73.
[34] C.A. Helm, L.A. Laxhuber, M. Lösche, H. Möhwald, J. Colloid Polym. Sci. 264 (1986) 46.
[35] M. Lösche, H.-P. Duwe, H. Möhwald, J. Colloid Interf. Sci. 126 (1988) 432.
[36] K. Kjaer, J. Als-Nielsen, C.A. Helm, L.A. Laxhuber, H. Möhwald, Phys. Rev. Lett. 58 (1987) 2224.
[37] B. Wetzer, A. Pfandler, E. Györvary, D. Pum, M. Lösche, U.B. Sleytr, Langmuir 14 (1998) 6899.
[38] M. Weygand, M. Schalke, P.B. Howes, K. Kjaer, J. Friedmann, B. Wetzer, D. Pum, U.B. Sleytr, M. Lösche, J. Mater. Chem. 10 (2000) 141.
[39] J. SkovPedersen, I.W. Hamley, Physica B198 (1994) 16.
[40] G. Büldt, H.U. Gally, A. Seelig, J. Seelig, Nature 271 (1978) 182.
[41] C.R. Flach, J.W. Brauner, R. Mendelsohn, Biophys. J. 65 (1993) 1994.